Spectroscopic Studies on Organometallic Schiff Base, Some Transition Metal Ion Complexes: Structural Insights and Anti-Microbial Activity

Priyanka S Thakur and Manohar V. Lokhande*

Department of Chemistry, Sathaye College (Autonomous), Mumbai – 400057, Maharashtra, India.

Abstract

The General formula [ML)·xH_2O] (where M = Mn(II), Ni(II), Co(II), Cu(II), and Pt(II); L = 2,2′-{(1R,1′S)-1,1′-ferrocen-2,4-dien-1-yl-2,2′-diyl bis[(Z)methyl-ylidenenitrilo]} bis(3-iodophenol)) has been successfully synthesised unique organometallic Schiff base complexes. Elemental analysis, magnetic susceptibility tests, conductivity investigations, IR spectroscopy, UV–visible spectroscopy, Electronic Spectra, SEM/ EDX mass spectrometry, and thermal analysis (TGA/DTA) were all used to characterise these complexes. Through the azomethine nitrogen (>C=N–) and hydroxyl oxygen atoms, the Schiff base ligand functions as a tetradentate donor. The resultant complexes have a coordination number of six and display octahedral geometry. To assess bonding qualities, electronic spectra were collected, and parameters such as the nephelauxetic effect (β), bonding parameter (b½), and Sinha's parameter (δ%) were calculated. Weight loss related to exothermic and endothermic processes was found in thermal investigations (TGA/DTA) of [Ni ($C_{36}H_{26}Fe_2N_4O_2$)] , and [Pt ($C_{36}H_{26}Fe_2N_4O_2$)] complexes. Furthermore, Cu(II) complex organometallic nanoparticles (OMNPs) were prepared. Particle sizes ranging from 25 to 57 nm were found by SEM and EDX characterisation. Three pathogenic fungi, Alternaria brassicae, Aspergillus niger, and Fusarium oxysporum, were used to test the ligand and its complexes for antifungal activity.

Key Words

FTIR, UV-Visible, TGA/DTA, SEM, EDX

1.0 Introduction

Organometallic Schiff base metal complexes have been identified as important components of biological systems [1-2]. Due to their numerous applications, these compounds are utilised in the polymer, dye, and pharmaceutical industries [3–4]. Additionally, it has been demonstrated that several organometallic Schiff base complexes exhibit luminescent properties [5-7]. Transition metal complexes made from organometallic Schiff bases have shown antitumor and anticancer properties [8–9], and other research has emphasised their potential for use in medicine. The fungicidal and insecticidal characteristics of these complexes have been thoroughly studied from a biological standpoint [10–12]. Additionally, as model compounds for researching the mechanism of reversible oxygenation, synthetic reversible oxygen-carrying complexes based on organometallic Schiff bases are particularly interesting [13–14]. These studies offer important information on how natural oxygen carriers, such as haemoglobin, operate [15].

In the field of medicine, organometallic compounds and metal complexes are becoming more and more significant as their medicinal qualities are investigated for the treatment of a variety of illnesses. The existence of one or more covalent metal–carbon bonds and their exceptional structural variety are characteristics of organometallic compounds. They are often uncharged, somewhat lipophilic, and kinetically stable, making them attractive options for the creation of new therapeutic medicines [16–18].In contrast, metal complexes are made up of a core metallic atom or ion that is attached to nearby molecules or ions. Both metal complexes and organometallic compounds have been shown to have anti-inflammatory properties and to be useful in reducing the negative effects of free radicals [19–20]. This study used elemental analysis, magnetic susceptibility, and spectrum analysis to characterise the synthesis of Schiff base molecules and some transitional metal ion complexes.

2.0 Material and Methods

Every chemical and reagent utilised was of analytical grade and didn't require any additional purification. AMI Chemicals provided the ferrocene dialdehyde chemical. Before usage, each solvent was distilled and purified. At IICT, elemental analysis was carried out. An Elico conductivity bridge was used in the college lab to assess conductivity. As a calibrant, [Hg Co $(CNS)_4$] was used to test magnetic susceptibility. KBr pellets were used to record infrared spectra on a Perkin-Elmer Paragon-500 spectrophotometer. The laboratory provided the mass spectra of the organometallic Schiff base and the synthesised complexes. A Cintra-5 GBC UV–Visible spectrophotometer was used to record electronic spectra. A Joel-8030 double goniometer X-ray powder diffractometer was used to gather X-ray powder diffraction (XRD) patterns. Toluene was used as the solvent in a specific gravity bottle to measure the densities of the complexes. On a Mettler Toledo Star system, thermogravimetric (TGA) and differential thermal analyses (DTA) were carried out in a nitrogen atmosphere between 25 and 900 °C. Atomic absorption spectroscopy (AAS) was used to determine the Pd(II) concentrations, whilst gravimetric analysis was used to quantify the iron amount.

2.1 Preparation of Organometallic Schiff Base Compound

1’1'-ferrocen-2, 4-dien-1-yl-2, 2'-dicarbaldehyde (1.45g) and 2-amino-3-iodophenol (2.04g) were dissolved independently in $20cm^3$ of ethanol and combined in an equimolar ratio. Two to three drops of alcoholic ammonia were added and mixed rapidly on a magnetic plate for thirty minutes. The resultant solutions were stored in a microwave oven for 10 minutes. This solution will then be allowed to cool overnight in a dark place until the solid separates. Whatman 41 filter paper is used to filter the solids. The product's yield percentage is 71%.

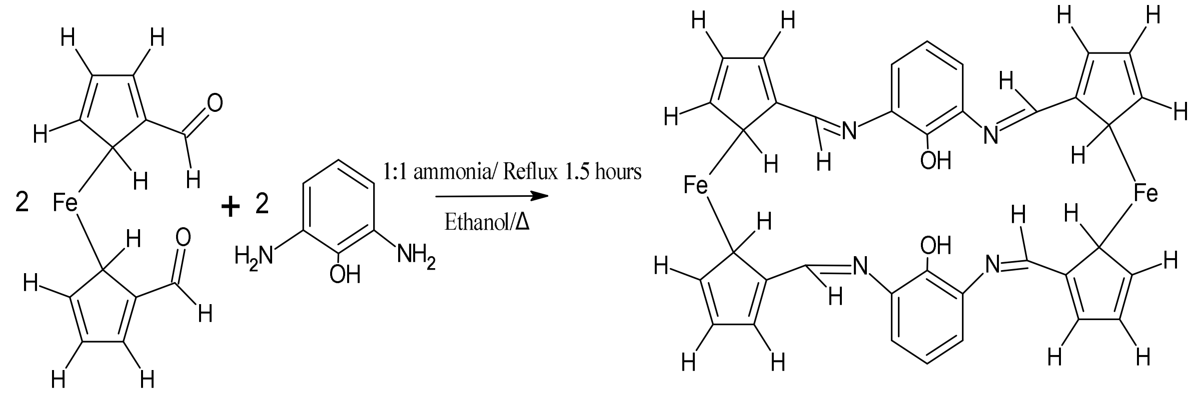

1,1′-Ferrocenedicarboxaldehyde 2,6-diaminophenol N,N′-[2-hydroxy-1,3-phenylenebis(azan-1-yl-1-ylidene)]bis(1′-formylferrocene)

2.2 Physical Properties of Schiff Base

Appearance	Reddish yellow crystalline powder
Molecular Formula	$C_{36}H_{28}Fe_2N_4O_2$
Molecular weight	660.336
Decomposition point (DP)	182-185 ºC

2.3 Metal Complex synthesis

The Schiff base ligand (L) dissolved in (Methanol + Isobutyl Alcohol), and A 0.2 M solution of metal chloride was prepared using double-distilled water. Equimolar solutions of the Schiff base (L) (0.2 M) and the metal chloride (0.2 M) were mixed in M:L ratios of 1:1, 2:1, and 1:2, and the resulting solutions were heated on a hot plate for sixty minutes with constant magnetic stirring. During the stirring, two to three drops of alcoholic ammonia were added. After sixty minutes of stirring, the mixture was kept in a hot microwave oven for roughly fifteen minutes. Kept in a dark place overnight, the solid reappeared. It was filtered, cleaned with alcohol, and dried for 12 hours at 60 °C in a dry oven. The product yield ranges from 48-59%.

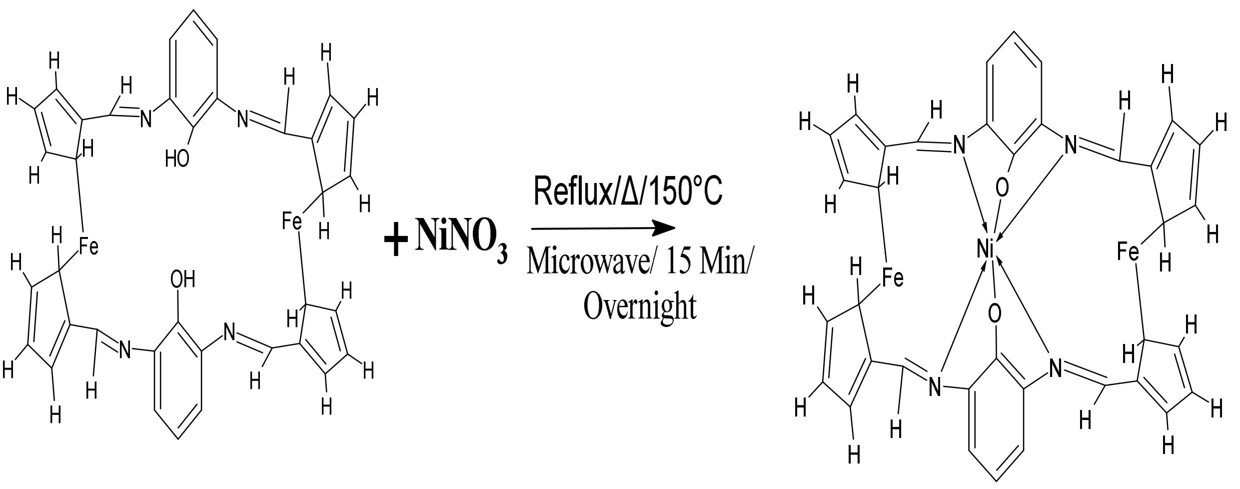

3.0 Results and Discussion

The produced compounds are stable at room temperature and are non-hygroscopic. On heating, they decompose at high temperatures. The complexes dissolve in DMF/DMSO but are insoluble in water. Table 1 provides a summary of the physical characteristics and analytical data. At room temperature, every compound that has been prepared is stable and colourful. The complexes are soluble in dimethyl sulfoxide and dimethyl formamide but insoluble in organic solvents such as toluene, methanol, ethanol, acetonitrile, and chloroform. They decompose in the range 205-230°C. The melting point and decomposition point reported in the open capillary are uncorrected. The complexes were non-electrolytic in nature [21], and their conductivity values were measured in a 10^{-3} molar solution of dimethyl sulfoxide [22].

The metal contents were estimated by using EDTA (0.01) with Xylenol Orange indicator for Fe^{3+} determination in an acidic medium. Murexide indicator is used for the estimation of Cobalt (II), $Cu^{2+}$and Ni^{2+} metal ions. Eriochrome Black T (EBT) is used for the estimation of Zn^{2+}metal ion and Cobalt ions. Platinum metal is estimated by using AAS.

Table -1: Analytical and Physical Data (* Experimental)

Complexes/Ligand	MP/ DP °C	% Yield	C%	H%	N%	Fe%	M%	Conductivity	**μ_{eff} BM**
($C_{36}H_{28}Fe_2N_4O_2$)	182-185	71 %	65.48	4.27	8.48	16.91	-	-	-
			65.01*	4.01*	8.25*	16.72*	-		
[Mn($C_{36}H_{26}Fe_2N_4O_2$)]	201-204	57%	56.86	3.67	7.86	15.66	7.70	4.28	5.09
			56.78*	3.55*	7.70*	15.48*	7.55*		
[Ni ($C_{36}H_{26}Fe_2N_4O_2$)]	215-218	54%	60.30	3.66	7.81	15.58	7.81	4.39	3.12
			60.15*	3.54*	7.69*	15.47*	7.69*		
[Co($C_{36}H_{26}Fe_2N_4O_2$)]	217-220	48%	60.28	3.65	7.81	15.57	8.22	4.55	4.48
			60.17*	3.55*	7.65*	15.44*	8.01*		
[Cu($C_{36}H_{26}Fe_2N_4O_2$)]	222-225	55%	59.90	3.63	7.76	15.47	8.80	4.69	2.11
			59.77*	3.54*	7.65*	15.35*	8.72*		
[Zn($C_{36}H_{26}Fe_2N_4O_2$)]	208-211	58%	59.75	3.62	7.74	15.43	9.04	4.77	Dimag
			59.63*	3.54*	7.60*	15.30*	8.95*		
[Pt($C_{36}H_{26}Fe_2N_4O_2$)]	225-228	51%	50.67	3.07	6.57	13.09	22.86	4.92	-
			50.60*	2.92*	6.42*	12.95*	22.74*		

3.1 Magnetic Properties

The complexes' corrected magnetic moment (μeff) in Bohr magnetons (BM) units. The magnetic moments of the complexes are measured at room temperature [23]. This suggests that the third electron plays a little role in the creation of bonds. Table -1 lists the complexes' μ_{eff}. values.

3.2 Ligand's Infrared Spectra

The infrared spectra of the ligand exhibit a band at 1645cm^{-1}, which is related to v(>C=N-) of the azomethine group [24]. The broad band in the area 3440-3450cm^{-1} is equivalent to v(O—H) hydroxyl groups. The IR spectra of the ligand exhibit the bands at 1650-1655 cm $^{-1}$, which relate towards the presence of v(C-H) and v(C=N). The (C-O) bands typically appear as a strong peak between 1170-1180 cm^{-1}, and the band at 450- 460 cm^{-1} is for the Fe-Cp ring, respectively [25].

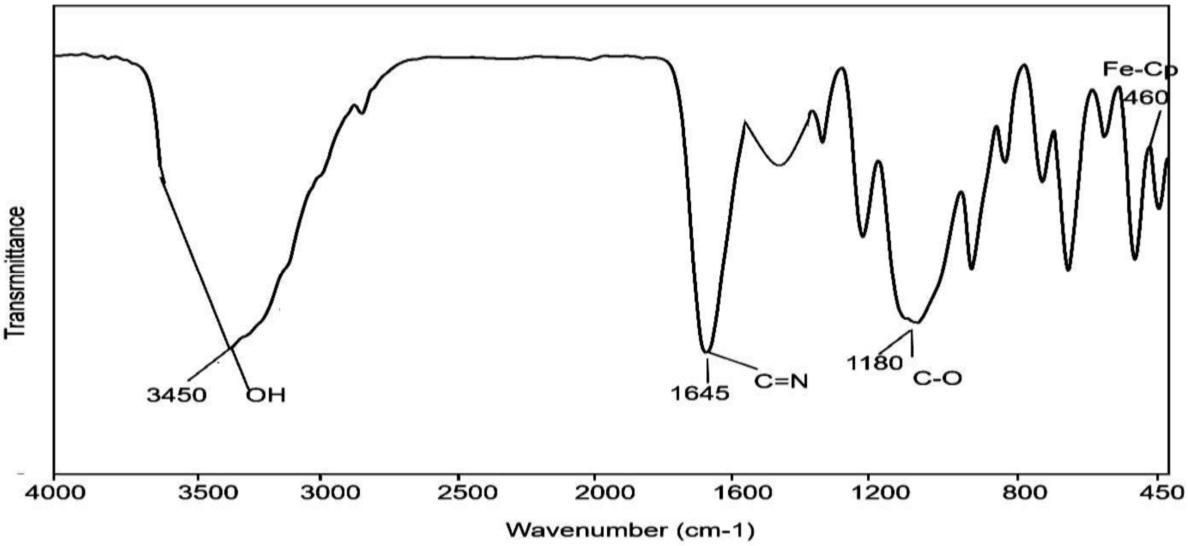

Figure-1: FTIR of Schiff Base Ligand

3.3 Infrared Spectra of the Metal Ion Complexes

The IR spectra provide vital information regarding the kind of functional group bound to the metal atom. To examine the bonding mode of Schiff bases to metal complexes. Relevant IR bands that give strong structural evidence for the production of ligand and complexes are described in Table 2 and in the figure. The infrared spectra of complexes were examined with the ligand and their substituted moieties [26]. All metal complexes' infrared band assignments show broad bands in the range 3475–3510 cm^{-1}, suggesting the presence of coordinated water molecules [27]. A band shifted in the low region at 1605-1625cm^{-1} is due to v (>C = N-) vibrations. The shifting of this group to a lower frequency in the metal complexes when compared to the free ligand suggests the coordination of the metal ion through the nitrogen atom of the azomethine group with the metal atom would reduce the electron density in the azomethine link and thus lower the –HC=N absorption [28]. A broad band at 3450cm^{-1} was seen in the spectra of the ligands due to υ(OH) stretching vibrations however this band disappeared in the spectra of all the complexes [29]; instead, a new band formed at 1235-1250 cm^{-1} due to the υ(>C-O) frequency, which clearly supports the fact that during chelation, deprotonation of the hydroxyl group [30]. The presence of nitrogen and oxygen atoms in conjunction with metal ions is supported by the appearance of new bands in the spectra of complexes in the region of 510-535 cm^{-1}, which correspond to vM-N [31] and 470-490cm^{-1} to υ M-O vibrations[32]. These bands are absent from the ligand spectrum.

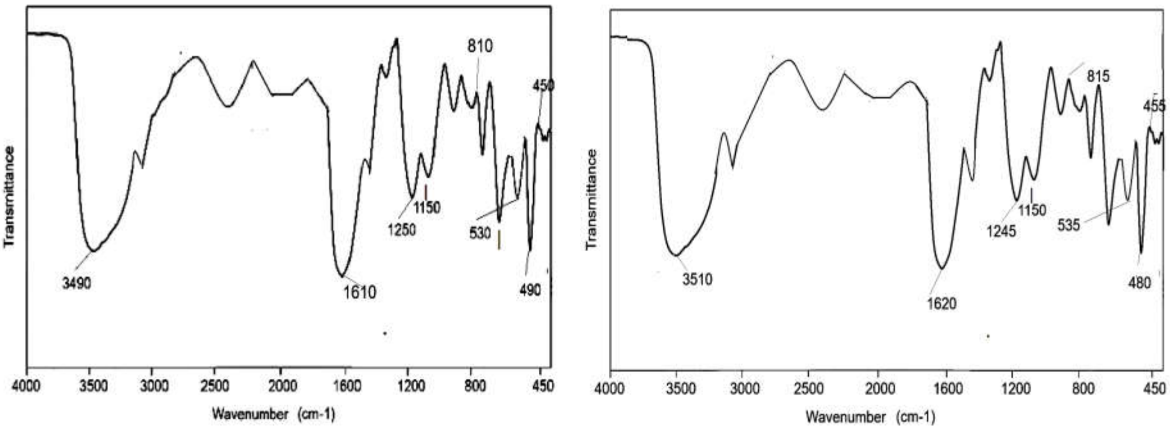

Figure 2: FTIR of Mn (II) and Co (II) Complexes

Table 2: FTIR of Schiff base ligand and metal complexes (in cm^{-1})

L/Complexes	**νOH**	**νHC=N**	**νH_2O**	**νH_2O**	**νNH_2**	**νM-O**	**νM-N**
$(C_{36}H_{28}Fe_2N_4O_2)$	3450	1645	-	-	3270	-	-
$[Mn(C_{36}H_{26}Fe_2N_4O_2)]$	-	1610	3490	3475	-	490	530
$[Co(C_{36}H_{26}Fe_2N_4O_2)]$	-	1620	3510	3495	-	480	535
$[Ni\ (C_{36}H_{26}Fe_2N_4O_2)]$	-	1610	3495	3480	-	485	525
$[Cu\ (C_{36}H_{26}Fe_2N_4O_2)]$	-	1612	3492	3484	-	479	525
$[Zn\ (C_{36}H_{26}Fe_2N_4O_2)]$	-	1618	3488	3475	-	485	528
$[Pt\ (C_{36}H_{26}Fe_2N_4O_2)]$	-	1621	3491	3471	-	487	527

3.4 Electronic Spectra

The electronic spectra of the Cu^{+2} and Ni^{+2} metal ion complexes have been recorded in DMF solutions in the wavelength range 380-800nm. The spectral parameters and their assignment are provided in Table 3. The electronic d-d transition bands generally display modest disruption due to complexation, with an increase in intensity, a shift to the red area, and the splitting of some bands observed upon complex creation. Ethanol and dimethyl sulfoxide are used in the solution phase to observe the position shapes of Cu^{+2} and Ni^{+2} ions. The Cu^{+2} and Ni^{+2} complexes have lower energies than those of the aqua complex. In Ni(II) complex UV region (345 nm): Strong LMCT and π–π* transitions. Visible region (425 nm): Weak d–d transitions, diagnostic of geometry. And Near IR (710): Additional d–d transitions I n octahedral complexes. In Cu (II) Complex MLCT (Cu → Ligand) peak at 385nm due to the possibility of π-acceptor ligands and d–d transitions at 520nm, Weak, broad, geometry-dependent. The extent of the bathochromic shift of the bands in each case, meagre Nephelauxetic effect (β) [33], the bonding parameter (b$^{1/2}$) [34] and Sinha's parameter (δ%) [35] were calculated. The 3d orbital's participation is reflected in the bonding parameter. A diminishing sequence of 3d–orbital participation in the Cu^{+2} and Ni^{+2} complexes is indicated by the b$^{1/2}$ value found for the current complexes. The average value of Sinha's parameter (δ% %) and η determined in each example is positive and lower, indicating the presence of weak covalent bonding character in the complexes.

Table 3: Electronic Spectra

Complexes	**Bands(nm)**	**β**	**1-β**	**η**	**$b^{1/2}$**	**δ %**
$[Ni(C_{36}H_{25}Fe_2N_4O_{2.})2H_2O]$	**425,610**	0.9835	0.0165	0.1289	0.0642	1.2952
$[Cu(C_{36}H_{25}Fe_2N_4O_{2.})2H_2O]$	**385, 520**	0.9795	0.0205	0.1439	0.0715	1.4466

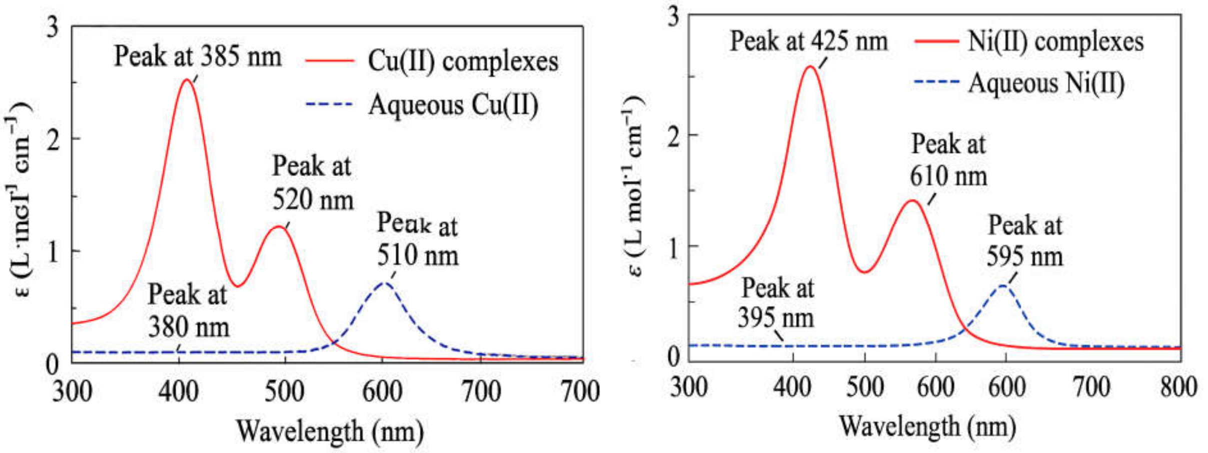

Figure -3: Electronic Spectra of Ni and Cu(II) Complexes

3.5 Thermal Analysis

The findings of the thermogravimetric and differential thermal analyses of $[Ni\ (C_{36}H_{26}Fe_2N_4O_2)]$, and $[Pt\ (C_{36}H_{26}Fe_2N_4O_2)]$ are presented below. Complexes lose weight owing to exothermic and endothermic activity [36-37]. These compounds break down in four stages and are thermally stable at room temperature. It is discovered from the figure that the heating rates were properly controlled at 20 °C min^{-1} under a nitrogen environment, and the weight loss was measured from the ambient temperature up to 800 °C. The schemes of the respective complexes are provided below.

Table 4: Thermogravimetric Data of Complex (* Exothermic)

Complex	**Temp. Range (°C)**	**Calculated value (%)**	**Experimental value (%)**	**Possible leaving groups**
$[Ni\ (C_{36}H_{26}Fe_2N_4O_2)]$	10-150	7.48	7.32	H_2O, CH_2
	150-325	19.12	18.98	H_2O, $C_5H_2N_2$
	325-490	21.42	21.28*	C_4H_6N
	500-900	39.45	39.335	Ni- Oxide
$[Pt\ (C_{36}H_{26}Fe_2N_4O_2)]$	10-160	8.12	8.02	H_2O, CH_2
	190-325	18.52	18.40	H_2O, C_5H_2N
	330-470	22.50	22.38*	$C_6H_5N_2$
	450-900	40.18	40.05	Pt-Oxide

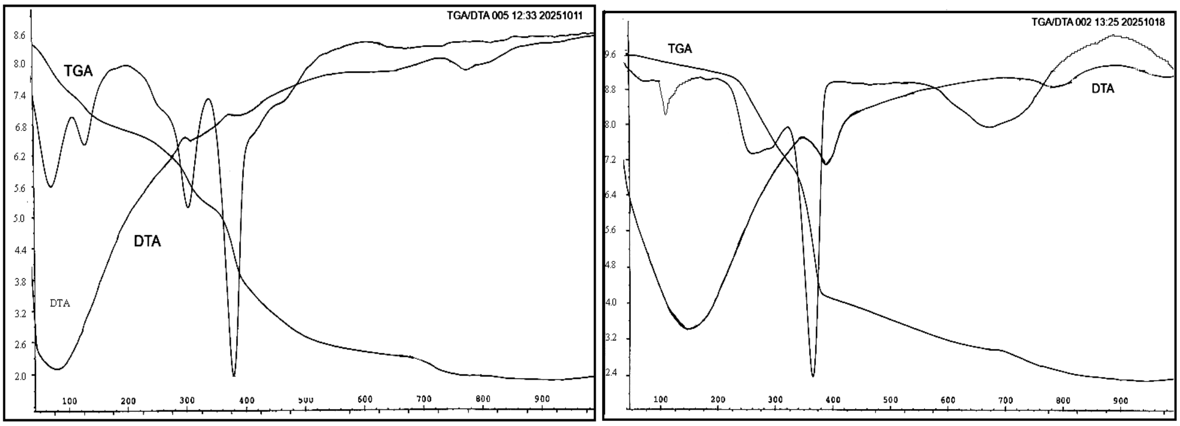

Figure -4: TGA/DTA of Ni(II) and Pt)II) Complexes

3.6 Synthesis of nanoparticles: Equimolar concentrations of ligand and metal solutions were mixed in the absence of ammonia and subjected to centrifugation at 6000 rpm for three hours. Post-centrifugation, the supernatant was concentrated to yield copper nanoparticles (CuNPs). Figure-5 presents the SEM and EDX analyses of the [Mn ($C_{36}H_{26}Fe_2N_4O_2$)] complex. The synthesised nanoparticles were subsequently subjected to further characterisation. SEM and EDX spectra of the resulting MnNPs were recorded, revealing particle sizes in the range of 25-57 nm.

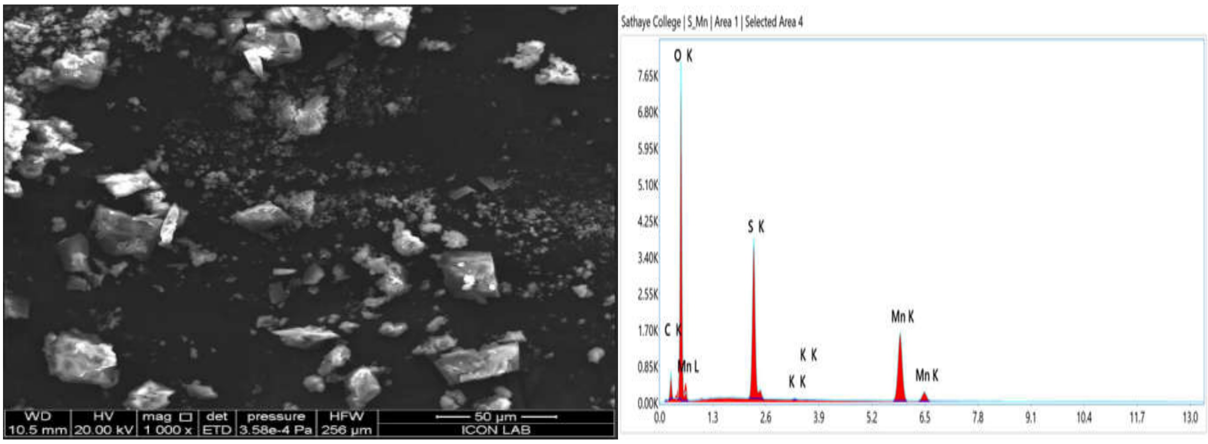

Figure -5: SEM and EDX of MnNPs

3.7 Antifungal Activity: The produced organometallic Schiff base ligand and its complexes were investigated for their antifungal activity against fungal strains identified as Alternaria brassicae, Aspergillus niger, and Fusarium oxysporum. The ligands and their complexes demonstrate varying anti-fungal effects against the fungal strains [38-39]. In comparison to unbound Schiff bases, their metal complexes demonstrated markedly stronger antibacterial activity. This enhanced effectiveness is likely due to the complexes' capacity to interfere with microbial cellular functions, making them more cytotoxic than the free ligands under equivalent experimental conditions. The observation is consistent with Tweedy's chelation theory, which suggests that chelation reduces the polarity of the metal ion through partial charge sharing with donor atoms and possible π-electron delocalisation across the chelate ring. These interactions can increase the ability of the complexes to penetrate microbial membranes, thereby boosting their antibacterial efficacy. Overall, the findings reveal a concentration-dependent rise in microbial inhibition with the use of metal complexes.

Table-5: Antifungal Activity

Ligand/ Complexes	**Alternaria brassicae**	**Aspergillus niger**	**Fusarium oxysporum**
Ligand	14	16	19
Mn (II)	22	19	23
Ni(II)	25	17	20
Co(II)	24	19	21
Cu(II)	21	23	25
Zn(II)	22	21	27
Pt(II)	23	26	22

Furthermore, the mechanism of action of these compounds may involve the formation of hydrogen bonds via the azomethine nitrogen atom (>C=N) with the active sites of cellular constituents, thereby disrupting normal cellular processes.

4.0 Conclusions

The structures of the ligand and its metal complexes with Mn(II), Co(II), Ni(II), Cu(II), and Pt(II) have been elucidated. Analytical data confirm that all complexes exhibit a 1:1 metal-to-ligand stoichiometry and behave in a non-electrolytic nature. Spectroscopic evidence indicates that the ligand functions as a neutral hexadentate donor ligand, coordinating through the nitrogen atom of the imino group and the oxygen atoms of the hydroxyl groups. Based on analytical, molar conductance, magnetic, and spectral studies, these complexes are characterised by an octahedral geometry. The nanoparticles obtained display sizes ranging from 25-57 nm. Antifungal assays reveal that the biological activity of the ligand against the tested organism is significantly enhanced upon chelation with metal ions.

Acknowledgement

The authors express their gratitude to the Principal and HOD, Chemistry, Sathaye College, for providing laboratory space. The authors further thank the Department of Chemistry, Institute of Science, ICON Lab and IICT for the necessary facilities.

Declaration of competing interest

The authors declare that they have no known competing financial interests or personal relationships that could have appeared to influence the work reported in this paper.

Data Availability Statement

The original contributions presented in the study are included in the article/Supplementary Material. Further inquiries can be directed to the corresponding author.

REFERENCE

1. Zoubi, W.A.; Ko, Y.G. *Organometallic complexes of Schiff bases: Recent progress in oxidation catalysis.* J. Organometal. Chem. 2016, 822(1), 173-188.https://doi.org/10.1016/j.jorganchem.2016.08.023
2. Liu,X .; Haman, J. *Recent developments in penta-, hexa- and heptadentate Schiff base ligands and their metal complexes*.Coord. Chem. Rev. 2019, 389, 94-118 .https:// doi. org/10.1016/j.ccr.2019.03.010
3. Farooq, M.G.; Lokhande, M.V. *Synthesis of ferrocene-based organometallic compounds & antimicrobial activity.* J. Appl. Chem. 2014, **7,** 2278-5736.
4. Boulechfar, C.; et.al. *Schiff bases and their metal Complexes: A review on the history, synthesis, and applications*.Inorg. Chem. Commu. 2023, 150, 110451. https://doi.org/10.1016/ j.inoche.2023.110451
5. Abu-Dief, A.M.; Mohamed I.M.A. *A review on versatile applications of transition metal complexes incorporating Schiff bases. J. Basic, Appl. Sci. 2015, 4(2),119-133. https://doi.org/10.1016/j.bjbas.2015.05.004*
6. Nishal,V.; et.al. *Characterisation and luminescent properties of zinc–Schiff base complexes for organic white light-emitting devices.* Cog.Chem.2015, 1, 1079291.*https://doi.org/10.1080/23312009.2015.1079291*
7. Aazam, E. S.; Husseiny, A. F. E. L.; Al-Amri, H. M. *Synthesis and photoluminescent properties of a Schiff-base ligand and its mononuclear Zn(II), Cd(II), Cu(II), Ni(II) and Pd(II) metal complexes.* Arab. J. Chem.2012, 5, 45–53. https://doi.org/10.1016/j.arabjc.2010.07.022
8. Lin, L.; Zheng, T.; Tang,L.; Wang,Z.; Liu,W. *Recent advances of Schiff base metal complexes as potential anticancer agents.* Coord. Chem. Rev.2025, 525, 216327.https://doi.org/10.1016/j.ccr.2024.216327
9. Wang,Y.; Wang, J.; Mou,L.; Zhang, H.; Chen, G.; Zhou ,C. *Comprehensive Insights Into Sulfanilamide-Based Medicinal Design and Research.* Med.Res.Rev.2025, 45(45), 1700-1817. https://doi.org/10.1002/med.22115.
10. Batawale, P.P.; Kapade, M.G.; Raut, U.M.; Lokhande, M.V. *Synthesis of Schiff base ligand, its novel Mn (II), Co (II), Ni (II), Cu (II), Zn (II), Pd (II) complexes: spectral investigation, biological applications, and Nanoparticles.* JZU Natural Sci.2025, 56(11), 267-273. https://doi.org/10.5996/jzund.2025.v25i8.23268
11. Wilkinson, S.M.; Sheedy, T.M.; New, E.J. *Synthesis and Characterisation of Metal Complexes with Schiff Base Ligands.* J Chem. Educ. 2016, 93(2):,351–354. https://doi.org/10.1021/acs.jchemed.5b00555
12. Santana-Romo, f.; Peñaherrera, J.L.; Sanchez,J.S.; Carreño-Otero, A.L.*Chemical-computational comparison of organometallic complexes in oxygen carriers and their incidence on blood colour*. Invest. Desarrollo.2023, 18(1),01-16. https://doi.org/10.31243/id.v18.2023.2176.
13. Ali, A.; Soman, S. S.; Vijayan, R. *Dynamics of camel and human haemoglobin revealed by molecular simulations.* Scientific Reports.2022, *12*(1), 122. https://doi.org/10.1038/s41598-021-04112-y,
14. Kapade, M.G.; Batawale, P.P.; Dalvi, U.M.; Lokhande, M.V. *Synthesis and Characterization of Noval Schiff Base Complexes Of Mn(II), Co(II), Ni(II), Cu(II), Zn(II), Pd(II), Pt(II) Metal Ions For Microbial Activities and Their Nanoparticles.* Inter J Pharm

Sci Res. 2024, 15(11), 3297-3306. https://doi.org/10.13040/IJPSR.0975-8232.15(11).3297-06

15. Gupta, A.S. *Haemoglobin-Based Oxygen Carriers: Current State-of-The-Art and Novel Molecules.* Shock. 2019,52(1),70–83. https://doi.org/10.1097/SHK.0000000000001009.
16. Shah, R. M.; Jadhav, S.R.; Bryant, G.; Kaur, I.P.; *Harding, I.H. On the formation and stability mechanisms of diverse lipid-based nanostructures for drug delivery.* Adv. Colloid. Inter. Sci.2025,338, 103402.https://doi.org/10.1016/j.cis.2025.103402.
17. Rehman, U.R.; Farid, A.; Shah, S.U.; Dar,M.J.; Rehman, A.U.Ahmed, N.;et. al. *Self-Emulsifying Drug Delivery Systems (SEDDS): Measuring Energy Dynamics to Determine Thermodynamic and Kinetic Stability.* Pharmaceuticals. **2022**, 15, 1064. https://doi.org/10.3390/ph15091064.
18. Dalmolin L.F.; Lopez, R. V.F. *Nanoemulsion as a Platform for Iontophoretic Delivery of Lipophilic Drugs in Skin Tumours.* Pharmaceutics**.** 2018, 10(4), 214; https://doi.org/10.3390/pharmaceutics10040214.
19. Chandimali, N.; Bak, S.Y.; Park, E.H.; Hyung-Jin, L.; Yeong-Seon, W.; Eun-Kyung, K.; Sang-Ik, P.; Lee, S.J. *Free radicals and their impact on health and antioxidant defences: a review.* Cell. Death. Disc.2025,11,1-19. https://doi.org/10.1038/s41420-024-02278-8.
20. Divya, C. *Comparative Study of Synthetic vs. Natural Antioxidants in Inflammatory Diseases.* Eur. J. Cardiovasc. Med.2019, 9(4), 65-68.
21. Krestov, G.A. *Thermodynamics of dissolution of non-electrolytes and electrolytes in non-aqueous solvents. J. Ther. Analy.* 1988, 33, 29–36. https://doi.org/10.1007/BF01914581.
22. Abdalla, E.M.; Hassan, S.S.; Elganzory, H.H.; Aly, S.A.; Alshater, H. *Molecular Docking, DFT Calculations, Effect of High Energetic Ionising Radiation, and Biological Evaluation of Some Novel Metal (II) Heteroleptic Complexes Bearing the Thiosemicarbazone Ligand.* Molecules. 2021, 26, 5851. https://doi.org/10.3390/molecules26195851.
23. Rao, T.R.; Sahay, M.; Agarwal, R.C. *Magnetic and spectral studies on M-metal complexes of acetone(N-isopropylidene) tyrosyl hydrazone*. Proc. Indian Acad. Sci. (Chem. Sci.), 1985, 96(5-6), 525-534.
24. Kapade, M.G.; Batawale, P.P.; Raut, U.M.; Lokhande, M.V. *Synthesis, characterisation of 2-[(z)-{[6-amino-2-(4 chlorophenyl) pyrimidin-4-yl] imino} methyl]-4 nitrophenol Schiff base with Mn (II), Co (II), Ni (II), Cu (II), Zn (II), Pt (II) for their nanoparticle and antibacterial studies.* Rasayan. J. Chem .2024, **17**(4), 1426-1435. http://doi.org/10.31788/RJC.2024.1748925.
25. Nair, M.; Appukuttan, A.S. *Syntheses, Spectral, Surface Morphological and Gamma Ray Irradiation Studies of Some Oxomolybdenum (V) and Dioxo molybdenum (Vi) Complexes of an Azo Dye Derived from 4-Aminoantipyrine*. J. Korean. Chem. Soc. 2012, 56, 217–227.http://dx.doi.org/10.5012/jkcs.2012.56.2.217.
26. George, A.; Lokhande, M.V.; Bhusare, S.R. *Synthesis and Characterisation of Mn (II), Co (II), Ni (II), Cu (II) and Zn (II) complexes with 4-{(E)-[(2-chlorophenyl) imino] methyl} benzene-1, 2-diamine.* J Chem. Biol. Phy. Sci. 2011, 2 (1),137-145.
27. Davletshina, N.; Khabibullina,A.; Davletshin R.; Ivshin,K.; Kataeva, O.; Cherkasov, R. *FT-IR spectroscopic analyses of the complex formation process of phosphorylated betaines with* metal ions. J. Organometal. Chem.2021,951, 121996. https://doi.org/10.1016/j.jorganchem.2021.121996.
28. Dalvi, U.M.; Kapade, M.G.; Batawale, P.P.; Lokhande. M.V. Synthesis, *Spectral Characterisation of Schiff Base of Some Transitional Metal Ion Complexes, Biological Activity, and Nanoparticles*. Degrees Journal. 2025, 10(3), 68-81. https://doi.org/12.1789001.DEJ.
29. Mohamed, G.G.; Zayed, M.A.; Abdallah, S.M. *Metal complexes of a novel Schiff base derived from sulphametrole and valeraldehyde. Synthesis, spectral, thermal*

characterisation, and biological activity. J Molecular Struc. 2010, 979 (1-3), 62-71. https://doi.org/10.1016/j.molstruc.2010.06.002.

30. Clifton, L.; Wagner, N.A.; Phan, J.C. ; Fettinger, L. A.; Berben, P. P. *New Characterization of V{N(SiMe3)2}3: Reductions of Tris[bis(trimethylsilyl) amido] vanadium(III) and -chromium(III) To Afford the Reduced Metal(II) Anions [M{N(SiMe3)2}3]− (M = V and Cr).* Inorg. Chem. 2019, *58* (9) , 6095-6101. https://doi.org/10.1021/acs.inorgchem.9b00381
31. Pan, S.; Zhao, L.; Frenking, G. *Bonding in* $M(NHBMe)_2$ *and* $M[Mn(CO)_5]_2$ *complexes (M=Zn, Cd, Hg; NHBMe=*$(HCNMe)_2B$*): divalent group 12 metals with zero oxidation state.* Theo. Chem. Acc. 2021, 140, 69-77. https://doi.org/10.1007/s00214-021-02751-y.
32. Afsan, F.; Dalia, S.A.; Hossain, S.; Sarker, S.; Zahan, K.E. *Synthesis, Spectral and Thermal Characterisation of Selected Metal Complexes Containing Schiff Base Ligands with Antimicrobial Activities.* Asian. J. Chem. Sci. 2018, 4(3), 1-19. http://doi.org/10.9734/ajocs/2018/40913
33. Salehi,M.; Rahimifar, F.; Kubicki, M.; Asadi, A. *Structural, spectroscopic, electrochemical and antibacterial studies of some new nickel(II) Schiff base complexes.* Inorg. Chim. Acta. 2016,43, 28-35, https://doi.org/10.1016/j.ica.2015.12.016.
34. El-Shahawi, M. S. ; Al-Jahdali, M. S. ; Bashammakh, A. S. ; Al-Sibaai, A. A. ; Nassef, H. M. Spectroscopic and electrochemical characterisation of some Schiff base metal complexes containing benzoin moiety. Spectrochim. Acta Part A: Mol. Biomol. Spectr.2013, 113, 459-465. http://doi.org/10.1016/j.saa.2013.04.090
35. Singh, A.K.; Sinha, S.P.; Kumar,V.; Rai, S.S.; Sharma,S. *Nephelauxetic Effect of Telluro Ether Complexes of Co(II), Ni(II) and Cu(II*) .Asian. J. Chem.2011, 23(10), 4347-4350.
36. Mukasyan, A.S. *DTA/TGA-Based Methods.* Concise 2017, 93-95. https://doi.org/10.1016/B978-0-12-804173-4.00040-5.
37. El-Boutaybi, M.; et.al. *Synthesis, Characterisation, DFT, and Thermogravimetric Analysis of Neutral Co (II)/Pyrazole Complex, Catalytic Activity toward Catecholase and Phenoxazinone Oxidation.* Crystals, 2023, 13(2), 155-167. https://doi.org/10.3390/cryst13020155.
38. Chirinos, J.; Ibarra, D.; Morillo, Á.; Llovera, L.; González, T.; Zárraga, J.; Larreal, O.; Guerra, M. *Synthesis, Characterisation and Catecholase Biomimetic Activity of Novel Cobalt(II), Copper(II), and Iron(II) Complexes Bearing Phenylene-Bis-Benzimidazole Ligand*. Polyhedron 2021, 203, 115232.https://doi.org/10.1016/j.poly.2021.115232.
39. Fekri,R.; Salehi, M.; Asadi, A.; Kubicki,M. *Synthesis, characterisation, anticancer and antibacterial evaluation of Schiff base ligands derived from hydrazone and their transition metal complexes.* Inorg. Chim. Acta. 2019,484, 245-254.https://doi.org/10.1016/j.ica.2018.09.022

****